



aerosol_cci2
ATBD (AATSR, ADV)

REF : ATBD – ADV
ISSUE : 4.1
DATE : 21.04.2017
PAGE : I



ESA Climate Change Initiative
aerosol_cci

Algorithm Theoretical Basis Document (ATBD)
AATSR
AATSR Dual View Algorithm (ADV)

Version 4.1

Document reference: Aerosol_cci_FMI_v4.1.docx



aerosol_cci2
ATBD (AATSR, ADV)

REF : ATBD – ADV
ISSUE : 4.1
DATE : 21.04.2017
PAGE : II

DOCUMENT STATUS SHEET

	FUNCTION	NAME	DATE	SIGNATURE
LEAD AUTHOR	editor	Pekka Kolmonen, FMI	21.04.2017	
CONTRIBUTING AUTHORS		Larisa Sogacheva, FMI		
REVIEWED BY	Co-science leader leader	Gerrit de Leeuw, FMI	24.04.2017	
APPROVED BY	Technical officer (ESA)	Simon Pinnock		
ISSUED BY	Project manager	Thomas Holzer- Popp		



aerosol_cci2
ATBD (AATSR, ADV)

REF : ATBD – ADV
ISSUE : 4.1
DATE : 21.04.2017
PAGE : III

EXECUTIVE SUMMARY

This Algorithm Theoretical Basis Document (ATBD) describes the theoretical basis for the aerosol retrieval algorithm developed for AATSR by FMI for application over land and ocean. This algorithm is referred to as AATSR Dual View (ADV) because it uses both the forward and the nadir view provided by AATSR to eliminate the effects of land surface reflectance on the radiation received at the top of the atmosphere (TOA). Over ocean the surface reflectance is modelled and both views are used independently to retrieval aerosol properties. The aerosol properties retrieved are the aerosol optical depths at the wavelengths in the visible to near-infrared, and the Ångström exponent describing the wavelengths dependence of the AOD. This is achieved by fitting the reflectance spectra at TOA computed using a forward model, the radiative transfer model DAK (Double Adding KNMI), to the measured those derived directly from the AATSR radiance measurements. The forward model uses a number of aerosol models for which the optical properties are computed using a Mie code. Two aerosol components, usually a fine and a coarse mode component, are mixed and the mixing ratio is varies to obtain the optimum wavelengths dependence using a least-square routine. The mixing ratio of these two, pre-selected, aerosol components is provided as an output as well.

Detailed descriptions of the algorithm have been provided in the peer-reviewed literature and several PhD theses. In this ATBD the algorithm is described with reference to the literature for more detail.



aerosol_cci2
ATBD (AATSR, ADV)

REF : ATBD – ADV
ISSUE : 4.1
DATE : 21.04.2017
PAGE : IV

Issue	Date	Modified Items / Reason for Change
0.1	17.02.2011	First draft
1.0	20.02.2011	Corrections and addition of exec sum.
2.0	20.09.2012	Update with new Aerosol_cci findings
3.0	27.11.2014	Update with results from Aerosol_cciPhase 1
4.0	03.11.2015	Update after the first processing of the ATSR2/AATSR 17 year data set
4.1	21.04.2017	Minor updates with references



aerosol_cci2
ATBD (AATSR, ADV)

REF : ATBD – ADV
ISSUE : 4.1
DATE : 21.04.2017
PAGE : V

LIST OF TABLES

	<p style="text-align: center;">aerosol_cci2 ATBD (AATSR, ADV)</p>	<p>REF : ATBD – ADV ISSUE : 4.1 DATE : 21.04.2017 PAGE : VI</p>
---	---	---

LIST OF FIGURES



TABLE OF CONTENTS

DOCUMENT STATUS SHEET	II
EXECUTIVE SUMMARY	III
LIST OF TABLES	V
LIST OF FIGURES	VI
TABLE OF CONTENTS.....	VII
1. INTRODUCTION.....	9
1.1 Scope.....	9
1.1.1 Applicable Documents.....	9
1.1.2 Reference Documents.....	9
2. INSTRUMENT CHARACTERISTICS.....	12
3 SCOPE OF THE PROBLEM	13
4. SCIENTIFIC BACKGROUND	14
4.1 Over land algorithm	14
4.2 ASV algorithm for over ocean retrieval.....	16
4.1.1 The modelled TOA reflectance.....	16
4.1.2 Ocean reflectance modeling.....	16
5. IMPLEMENTATION.....	18
5.1 Over land implementation.....	18
5.2 Over ocean implementation	20
5.3 Cloud screening.....	20
5.4 Adaptation of ADV/ASV for global multi-year retrievals.....	21
5.5 Post processing - Additional cloud screening.....	22
6 ERROR ESTIMATION	24
6.1 Error estimation for ADV	24
6.2 Error estimation for ASV	1
7. INPUT DATA REQUIREMENTS	2
7.1 AATSR reflectance	2
7.2 Aerosol look-up-tables (LUTs)	2
7.3 Chlorophyll concentration.....	2
7.4 Monthly wind speed climatology.....	2
8. ALGORITHM OUTPUT	3
9. PRACTICAL CONSIDERATIONS FOR IMPLEMENTATION.....	4
9.1 The retrieval algorithm.....	4
9.2 Look-up-table (LUT) computation.....	4
10. CONCLUSIONS.....	5



aerosol_cci2
ATBD (AATSR, ADV)

REF : ATBD – ADV
ISSUE : 4.1
DATE : 21.04.2017
PAGE : VIII



1. INTRODUCTION

This document describes the theoretical basis for the aerosol retrieval algorithm developed for AATSR by FMI for application over land and ocean. The algorithm over land is referred to as AATSR Dual View (ADV) and the algorithm over ocean to as AAYST Single View (ASV). The algorithm forms the basis for further development and improvement in the Aerosol_cci project.

1.1 Scope

The ADV has been extensively described in a series of peer-reviewed papers and PhD theses. This ATBD aims to provide an overview of the algorithm with summaries of the issues that are important for the Aerosol_cci work. It will not be a comprehensive compilation of all existing literature.

1.1.1 Applicable Documents

- [AD1] Statement of Work “ESA CLimate Change Initiative Stage 1, Scientific user Consultation and Detailed Specification”, ref EOP-SEP/SOW/0031-09/SP. Issue 1.4, revision 1, dated 9 November, 2009, together with its Annex C “Aerosols” (altogether the SoW).
- [AD2] The Prime Contractor’s Baseline proposal, ref. 3003432, Revision 1.0, dated 16 June 2010, and the minutes of the July 26, 2010 kick-off meeting.
- [AD3] Aerosol_cci project management plan (PMP), version 1.3.

1.1.2 Reference Documents

- [1] AATSR Product Handbook, Issue 2.2, European Space Agency. Available at ESA AATSR internet site (<http://envisat.esa.int/handbooks/aatsr/>), 2007.
- [2] Abdou, W.A., Martonchik, J.V., Kahn, R.A., West, R.A., and Diner, D.J.: A modified linear-mixing method for calculating atmospheric path radiances of aerosol mixtures, *J. Geophys. Res.*, 102, 16883–16888, 1997.
- [3] Cox, C., W. Munk, Measurement of the roughness of the sea surface from photographs of the Sun’s glitter, *J. Opt. Soc. Am.*, 44, 838–850, 1954.
- [4] Curier, L., de Leeuw, G., Kolmonen, P., Sundström, A.-M., Sogacheva, L., and Bennouna, Y., Aerosol retrieval over land using the (A)ATSR dual-view algorithm, in *Satellite Aerosol Remote Sensing Over Land*, Kokhanovsky, A.A. and de Leeuw, G. (editors), Springer, Berlin, 2009.
- [5] de Haan, J.F., Bosma, P.B., and Hovenier, J.W., The adding method for multiple scattering computations of polarized light, *Astron. Astrophys.*, 183, 371–381, 1987.
- [6] Flowerdew, R.J. and Haigh, J.D., An approximation to improve accuracy in the derivation of surface reflectances from multi-look satellite radiometers, *Geophys. Res. Lett.*, 22, 1693–1696, 1995.
- [7] Gill, P.E., Murray W., and Wright, M.H, *Practical Optimization*, Academic Press, 1999.
- [8] Grey, W., North, P., and Los, S., Computationally efficient method for retrieving aerosol optical depth from ATSR-2 and AATSR data, *Appl. Optics*, 45, 2786–2795, 2006.



- [9] Heitzenberg, J., Properties of the log-normal particle size distribution, *Aerosol Science and Technology*, 21, 46–48, 1994.
- [10] Holben B.N., Eck, T.F., Slutsker, I., Tanr, D., Buis, J.P., Setzer, A., Vermote, E., Reagan, J.A., Kaufman, Y., Nakajima, T., Lavenu, F., Jankowiak, I., and Smirnov, A., AERONET - A federated instrument network and data archive for aerosol characterization, *Rem. Sens. Environ.*, 66, 1–16, 1998.
- [11] Ivanov, A. P., *Physical Properties of Hydro-optics*, Nauka i Tekhnika, Minsk, 1975.
- [12] Koelemeijer, R.B.A., Stammes, P., Hovenier, J.W., and de Haan, J.D., A fast method for retrieval of cloud parameters using oxygen A-band measurements from the Global Ozone Monitoring Instrument, *J. Geophys. Res.*, 106, 3475–3490, 2001.
- [13] Kokhanovsky, A.A., Curier R.L., Bennouna, Y., Schoemaker, R., de Leeuw, G., North, P.R.J., Grey, W.M.F., and Lee, K.-H., The inter-comparison of AATSR dual view aerosol optical thickness retrievals with results from various algorithms and instruments, *Int. J. Remote Sensing*, 30, 4525–4537, 2009.
- [14] Mie, G., Beiträge zur Optik trüber Medien, speziell kolloidaler Metallösungen, *Ann. Phys.*, 330, 377–445, 1908.
- [15] Meyer, S.L., *Data Analysis for Scientists and Engineers*, Wiley, 1975. [16] Mishchenko M.I., Travis L.D., and Mackowski D.W., T-matrix computations of light scattering by nonspherical particles: A review, *J. Quant. Spectrosc. Radiat. Transfer*, 55, 535–575, 1996.
- [17] Monado F.M., Li X., Pichel W.G., and Jackson C.R., Ocean wind speed climatology from spaceborne SAR imagery, *Bull. Amer. Meteor. Soc.*, 95, 565–569, 2013.
- [18] Monahan, E.C. and O’Muircheartaigh, I., Optimal power-law description of oceanic whitecap coverage dependence on wind speed, *J. Phys. Ocean.*, 10, 2094–2099, 1980.
- [19] Morel, A., Optical modeling of the upper ocean in relation to its biogeochemical matter content (case I waters), *J. Geophys. Res.*, 93, 10749–10768, 1988.
- [20] North, P.R.J., Briggs, S.A., Plummer, S.E. and Settle, J.J., Retrieval of land surface bidirectional reflectance and aerosol opacity from ATSR-2 multi-angle imagery, *IEEE Trans. Geosci. Remote Sens.*, 37, 526–537, 1999
- [21] Robles González, C., Veefkind, J.P., and de Leeuw, G., Mean aerosol optical depth over Europe in August 1997 derived from ATSR-2 data, *Geophys. Res. Lett.*, 27, 955–959, 2000.
- [22] Robles González, C., *Retrieval of Aerosol Properties Using ATSR-2 Observations and Their Interpretation*, Ph.D. thesis, University of Utrecht, 2003.
- [23] Robles González, C. and de Leeuw, G., Aerosol properties over the SAFARI-2000 area retrieved from ATSR-2, *J. Geophys. Res.*, 113, 2008.
- [24] Saunders, R.W. and Kriebel, K.T., An improved method for detecting clear sky and cloudy radiances from AVHRR data, *Int. J. Remote Sensing*, 9, 123–150, 1988.
- [25] Sundström, A.-M. Kolmonen, P., Sogacheva, L., and de Leeuw G., Aerosol retrievals over China with the AATSR Dual-View Algorithm, *Remote Sens. Environ.*, 2011.
- [26] Tarantola, A., *Inverse Problem Theory*, Elsevier, 1987.
- [27] Thomas, G.E., E. Carboni, A.M. Sayer, C.A. Poulsen, R. Siddans, R.G. Grainger, Oxford-RAL Aerosol and Cloud (ORAC): aerosol retrievals from satellite radiometers, in *Satellite Aerosol Remote Sensing Over Land*, A. A. Kokhanovsky and G. de Leeuw (eds.), Springer, 2009.
- [28] Veefkind, J.P., de Leeuw, G., A new algorithm to determine the spectral aerosol optical depth from satellite radiometer measurements, *J. Aerosol Sci.*, 29, 1237–1248, 1998.



aerosol_cci2
ATBD (AATSR, ADV)

REF : ATBD – ADV
ISSUE : 4.1
DATE : 21.04.2017
PAGE : XI

- [29] Veefkind, J.P., de Leeuw, G.D., and Durkee, P.A., Retrieval of aerosol optical depth over land using two-angle view satellite radiometry during TARFOX, *Geophys. Res. Lett.*, 25, 3135–3138, 1999.
- [30] Veefkind, J.P., de Leeuw, G.D., Stammes, P., and Koelemeijer, R.B.A., Regional distribution of aerosol over land, derived from ATSR-2 and GOME, *Remote Sens. Environ.*, 74, 377–386, 2000.
- [31] Wanner, W., Strahler, A.H., Hu, B., Lewis, P., Muller, J.-P., Li, X., Barker Schaaf, C.L., and Barnsley, M.J., Global retrieval of bidirectional reflectance and albedo over land from EOS MODIS and MISR data: theory and algorithm, *J. Geophys. Res.*, 102, 17143–17161, 1997.
- [32] Kolmonen, P., L. Sogacheva, T.H. Virtanen, G. de Leeuw and M. Kulmala (2016). The ADV/ASV AATSR aerosol retrieval algorithm: current status and presentation of a full-mission AOD data set. *International Journal of Digital Earth*, 9:6, 545-561, DOI: 10.1080/17538947.2015.1111450.
- [33] Sogacheva, L., Kolmonen, P., Virtanen, T. H., Rodriguez, E., Saponaro, G., and de Leeuw, G.: Post-processing to remove residual clouds from aerosol optical depth retrieved using the Advanced Along Track Scanning Radiometer, *Atmos. Meas. Tech.*, 10, 491-505, doi:10.5194/amt-10-491-2017, 2017.



2. INSTRUMENT CHARACTERISTICS

The Advanced Along-Track Scanning Radiometer (AATSR) instrument launched in 2002 onboard Envisat is the next in the series of ATSR instruments that were launched on the ERS-1 (ATSR-1) and ERS-2 (ATSR-2) platforms. ATSR-1 has not been used for aerosol retrieval. The ATSR-2, AATSR and the future SLSTA on Sentinel-3 provide a long-term global dataset starting in 1995 which is one of the benefits of the ATSR mission.

The ATSR and AATSR radiometers were designed for atmospheric, surface and land scientific applications. ATSR was developed to provide high-accuracy measurements of Sea Surface Temperature (SST) for use in studies of global climate change. The other objectives of those instruments are the land surface and vegetation properties observation; instruments are used for fire detection. However, since ATSR-2 and AATSR have visible and near-infrared channels, those instruments have also successfully been used for aerosol retrieval.

AATSR is a dual view instrument with an across-track conical scanning for both views, which are near-simultaneous in time. The time between the two views measurements is 150 seconds. The scan mirror detecting radiation is continuously rotation from two apertures and two onboard blackbody calibration targets onto the radiometer. One view is near nadir and the other one is at a 55° forward angle. By viewing the same point through different atmospheric paths, it is possible to estimate and correct for the effect of atmospheric and surface contribution.

The nominal resolution at nadir is 1x1 km² and the swath width is 512 km which results in global coverage in 5-6 days. AATSR has three wave bands in the visible – near infrared (centered near 0.555 μm, 659 μm, 865 μm) and four bands in the infrared (centered near 1.610 μm, 3.7 μm, 10.85 μm, 12.00 μm) channels.



3 SCOPE OF THE PROBLEM

The problem is stated as: retrieve aerosol properties globally using the measured TOA reflectance spectrum provided by the AATSR instrument.

The problem is divided into two separate parts:

1. The retrieval of aerosol optical depth (AOD) over land. This is achieved by using the dual view feature of the instrument to overcome the problem of unknown land surface reflectance.
2. The retrieval of AOD over ocean. Ocean surface is modeled with theoretical and empirical knowledge about the surface reflectance.

The primary retrieval result is AOD. It is, however, possible to determine derived products, such as Ångström exponent and land surface reflectance.



4. SCIENTIFIC BACKGROUND

The ADV algorithm uses the dual view feature of the AATSR instrument to treat surface reflectance over land. Ocean surface is modelled taking into account e.g. chlorophyll concentration. The current status has been described in detail in peer-reviewed publication [32, 33] and is briefly summarized in the chapters below.

4.1 Over land algorithm

The dual-view algorithm for the AATSR top-of-atmosphere (TOA) reflectance is meant for retrieval of aerosol optical properties over land [29, 30, 22, 4]. These properties include AOD for three wavelengths (nominally 0.555, 0.659 and 1.61 μm). In addition, an aerosol model is retrieved. The model is a mixture of four aerosol components each of which is described by a log-normal size distribution defined by an effective radius and standard deviation (see section 3.2), and a complex refractive index. Two of the aerosol components define small particles and the other two coarse particles. One of the small particle components is non-absorbing while the other is strongly absorbing. By mixing these two components the absorbance of the small particles arbitrary absorbing properties for the small particles can be set. The coarse particle components are sea salt and dust. Of the four components the dust one is determined by employing non-spherical particles. The final aerosol model is determined by first mixing the small and large components separately, and finally mixing the ensuing small and coarse models together.

The aerosol components are adopted from the ESA Aerosol CCI (Climate Change Initiative) project¹. The properties of the components are described in table 1. One of the needed mixtures, the dust fraction, is taken from the AEROCOM aerosol climatology. The non-absorbing fine – absorbing fine mixture is retrieved semi-freely. The mixture can have any value in the range of ± 0.3 from the AEROCOM climatology value. The fine – coarse mixture is retrieved completely independent of the climatology. The algorithm is based on a number of assumptions:

- TOA reflectance ρ is of the form (Veefkind et al. [30])

$$\rho(\mu_1, \mu, \varphi, \lambda) = \rho_a(\mu_1, \mu, \varphi, \lambda) + \frac{T(\mu_1, \mu, \varphi, \lambda) \rho_g(\mu_1, \mu, \varphi, \lambda)}{1 - s(\lambda) R_s(\lambda)}, \quad (4.1)$$

where ρ_a is the reflectance due to the atmosphere, ρ_g is the ground reflectance, T is the product of downward and upward atmospheric transmittance, s is the atmospheric backscatter ratio, and R_s is the surface albedo. Reflectance and transmittance parameters: μ_1 is the solar zenith angle, μ is the viewing (satellite) zenith angle, φ is the relative azimuth angle between the sun and the satellite, and λ is the wavelength. Note that multiple scattering between ground and atmosphere is assumed here to be angle-independent for method development purposes. It has also been suggested that multiple scattering in the surface-atmosphere system will lead to isotropically distributed scattering [31].

- Atmospheric reflectance

$$\rho_a(\mu_1, \mu, \varphi, \lambda) = \rho_R(\mu_1, \mu, \varphi, \lambda) + \rho_{\text{aer}}(\mu_1, \mu, \varphi, \lambda), \quad (4.2)$$



where ρ_R is reflectance due to Rayleigh scattering and ρ_{aer} is reflectance due to aerosols.

- Reflectance due to aerosols is computed using the modified linear mixing method by Abdou et al. [2]. The method as adapted to ADV is

$$\rho_{\text{aer}} = b_1 \frac{\omega_{\text{mix}}}{\omega_1} e^{-\tau_1 |\omega_1 - \omega_{\text{mix}}|} \rho_1 + b_2 \frac{\omega_{\text{mix}}}{\omega_2} e^{-\tau_2 |\omega_2 - \omega_{\text{mix}}|} \rho_2, \quad (4.3)$$

where ω is the single scattering albedo (SSA) and τ is AOD. Subscripts 1 and 2 refer to two aerosol types while mix refers to the linear mixture of the two types. For the weighing coefficients $b_1 + b_2 = 1$. The modified linear mixing method is applied to take better into account the effects of mixing two aerosols with different absorbing properties. This is done by introducing the single scattering albedo into linear mixing. If the SSAs of the two aerosol types are identical, equation (4.3) simplifies to

$$\rho_{\text{aer}} = b_1 \rho_1 + b_2 \rho_2. \quad (4.4)$$

The also needed aerosol transmittance is computed using linear mixing.

- The ratio k between the surface reflectance of the forward and nadir views is independent of wavelength [6]:

$$k = \frac{\rho_g^f(\mu_1, \mu, \varphi, \lambda)}{\rho_g^n(\mu_1, \mu, \varphi, \lambda)}, \quad (4.5)$$

where ρ_g^f and ρ_g^n are the forward and nadir surface reflectance, respectively. Also, because reflectance due to aerosols at $1.61 \mu\text{m}$ is small compared to surface reflectance, the k -ratio is computed using equation


$$k = \frac{\rho^f(\mu_1, \mu, \varphi, 1.61 \mu\text{m})}{\rho^n(\mu_1, \mu, \varphi, 1.61 \mu\text{m})}. \quad (4.6)$$

Coarse particles contribute to reflectance at IR wavelengths. This may cause some error in the k -ratio in, for instance, in heavy dust conditions.

- The $0.865 \mu\text{m}$ channel is excluded from the retrieval because the k -ratio assumption is usually not valid as there is a strong reflectance by vegetation at this wavelength [21].

The dual-view method for AOD retrieval is derived based on the above assumptions. Equation (4.1) can be written separately for the forward and nadir views. Then, by combining these equations while keeping in mind that the multiple scattering is assumed to be angle independent, relation

$$\frac{\rho^n(\mu_1, \mu, \varphi, \lambda) - \rho_a^n(\mu_1, \mu, \varphi, \lambda)}{\rho_g^n(\mu_1, \mu, \varphi, \lambda) T^n(\mu_1, \mu, \varphi, \lambda)} = \frac{\rho^f(\mu_1, \mu, \varphi, \lambda) - \rho_a^f(\mu_1, \mu, \varphi, \lambda)}{\rho_g^f(\mu_1, \mu, \varphi, \lambda) T^f(\mu_1, \mu, \varphi, \lambda)} \quad (4.7)$$

	aerosol_cci2 ATBD (AATSR, ADV)	REF : ATBD – ADV ISSUE : 4.1 DATE : 21.04.2017 PAGE : XVI
---	---	--

can be made formally. The key aspect of the dual-view algorithm is to introduce the k -ratio in equation (4.7) to obtain

$$\frac{\rho^n(\mu_1, \mu, \varphi, \lambda) - \rho_a^n(\mu_1, \mu, \varphi, \lambda)}{T^n(\mu_1, \mu, \varphi, \lambda)} = \frac{\rho^f(\mu_1, \mu, \varphi, \lambda) - \rho_a^f(\mu_1, \mu, \varphi, \lambda)}{kT^f(\mu_1, \mu, \varphi, \lambda)}. \quad (4.8)$$

Now all the needed knowledge about surface reflectance is in the k -ratio.

4.2 ASV algorithm for over ocean retrieval

The basic principle of the algorithm is to minimize the discrepancy between the TOA measured and modeled reflectance at wavelengths of 0.555, 0.659, 0865 and 1.61 μm . The modeled reflectance is described below.

4.1.1 The modelled TOA reflectance

The TOA reflectance over ocean is given by [28]:

$$\rho_{TOA} = \rho_a + T_{\downarrow} \rho_{s,dir} / (1 - S \times \rho_{s,dir}) T_{\uparrow} + t_{\downarrow} \rho_{s,dif\downarrow} T_{\uparrow} + T_{\downarrow} \rho_{s,dif\uparrow} t_{\uparrow} + t_{\downarrow} \rho_{s,iso} t_{\uparrow} \quad (4.9)$$

(a)
(b)
(c)
(d)
(e)

where ρ_{TOA} is the top-of-the atmosphere reflectance, S is the spherical albedo, T is the direct transmittance and t is the diffuse transmittance upwards (\uparrow) and downwards (\downarrow). The terms ρ_a and ρ_s are the atmospheric and surface reflectances, respectively, and the other terms come from the ocean surface model which is described in next section. The multiple scattering between surface and atmosphere has been included only for direct down – direct up case as it becomes negligible when diffuse transmittance is applied. Note that geometric and wavelength dependencies in equation (4.9) are omitted for brevity.

Explanation of the components of eq. (4.9):

- (a) Reflectance due to scattering in the atmosphere by aerosols and molecules.
- (b) Photons transmitted downward, reflected by the ocean surface, and transmitted up.
- (c) Photons scattered along the downward path, reflected by the ocean surface, and transmitted up.
- (d) Photons transmitted downward, reflected by the ocean surface, and scattered towards the satellite instrument.
- (e) Photons scattered along the downward path, reflected by the ocean surface, and scattered towards the satellite instrument.

Each of the terms in equation (4.9) contains contributions of specular (Fresnel) reflection, oceanic whitecaps and subsurface scattering.

4.1.2 Ocean reflectance modeling

The ocean surface reflectance is modelled as the sum of specular (Fresnel) reflectance [3], and reflectance by subsurface scattering. The Fresnel part is described by the geometric



situation while the subsurface scattering is a function of chlorophyll concentration. The surface reflectance is a sum of four components based on atmospheric transmittance (see equation 4.9). The reflectance in these components is given by:

$$\rho_{s,dir}(\mu_0, \mu, \varphi, \lambda) = \rho_{glint}(\mu_0, \mu, \varphi, \lambda) + \rho_{chl}(C, \lambda) \quad (4.10)$$

where ρ_{glint} is the sun glint and ρ_{chl} is the subsurface reflectance due to chlorophyll concentration C , and it is assumed here to be Lambertian [28]. In practice the reflectance due to sun glint is not taken into account because pixels flagged as sun glint in the AATSR L1 data are not used in the retrieval. The geometric situation is described by the cosine of solar zenith angle μ_0 , the cosine of viewing zenith angle, μ and the relative azimuth angle φ . Reflectance depends on the wavelength λ . Subsurface reflectance is modeled after Morel [19] for case I waters:

$$\rho_{s,dif\downarrow}(\mu_0, \mu, \varphi, \lambda) = \rho_{Fresnel}(\mu_0) + \rho_{chl}(C, \lambda) \quad (4.11)$$

$$\rho_{s,dif\uparrow}(\mu_0, \mu, \varphi, \lambda) = \rho_{Fresnel}(\mu) + \rho_{chl}(C, \lambda) \quad (4.12)$$

$$\rho_{s,iso}(\mu_0, \mu, \varphi, \lambda) = 0.066 + \rho_{chl}(C, \lambda). \quad (4.13)$$

In these equations $\rho_{Fresnel}$ is the Fresnel reflection, and the factor 0.066 has been adopted from [11]. The possible error caused by the approximate value is minimal because the contribution of the last term to the TOA reflectance is small.

All of the above components include the contribution of the whitecap reflectance determined by the fraction of the ocean surface covered by whitecaps. The whitecap fraction W is a function of wind speed U [18]:

$$W = 3.84 \times 10^{-6} \times U^{3.41} \quad (4.14)$$

5. IMPLEMENTATION

5.1 Over land implementation

Modeled values of the atmospheric reflectance ρ_a and transmittance T must be determined in order to use equation (4.8) for the retrieval of aerosol properties. These values, together with other information can be computed using a radiative transfer (RT) method. RT methods provide a way to solve the forward problem of the retrieval. The forward problem for the case of the atmospheric reflectance can be stated as: when the atmospheric conditions (aerosol and gas concentrations) are known determine the amount of light that is reflected from the atmosphere towards a satellite instrument. During a retrieval the forward problem must be solved numerous times which is time consuming. The most common technique to overcome this is to perform the radiative transfer calculations for a set of fixed variables before the retrieval. The calculated values are arranged into an array which is called a look-up-table (LUT). During the retrieval the needed values can then be interpolated quickly from the LUT. The chosen RT algorithm that is used with the ADV is the DAK (Doubling Adding KNMI [5]).

LUTs are computed for each aerosol component. The size distribution of an aerosol component is described by the log-normal number size distribution of the form


$$\frac{dN}{d\ln r} = \frac{N_0}{\ln \sigma \sqrt{2\pi}} \exp\left(-\frac{\ln^2(r/r_g)}{2\ln^2 \sigma}\right), \quad (5.1)$$

where r is the particle radius. The size distribution of an aerosol type is defined by the geometric mean radius r_g and standard deviation σ [9]. The total number of aerosol particles N_0 depends on the aerosol load. Aerosol optical properties are computed by applying Mie calculations [14] except for the used non-spherical dust component where T-matrix is used [16]. These calculations require the knowledge of the aerosol particle size distribution and refractive index. The aerosol components are described in table 1.

Table 5.1: The Aerosol CCI aerosol components. Listed are the geometric radius r_g , standard deviation σ , refractive index n , and the aerosol layer height (alh).

components	r_g (μm)	σ	n	alh (km)
non-absorbing fine	0.07	1.700	1.40 - 0.003i	0-2
absorbing fine	0.07	1.700	1.50 - 0.040i	0-2
sea salt	0.788	1.822	1.40 - 0.000i	0-1
dust	0.788	1.822	1.56 - 0.002i	2-4

The LUTs are computed for discrete sun zenith, viewing zenith and relative azimuth angles, for each AATSR wavelength, and for a number of reference AOD levels. Currently, for ADV, 15 discrete values ranging from 0° to 90° for zenith angles and 19 discrete values between 0° and 180° for azimuth angle are used. Typically, ten AOD levels ranging from 0.05 to 4.0 at $\lambda = 0.500 \mu\text{m}$ are used with the ADV. Transmittance and reflectance are computed also for Rayleigh (gas) scattering in standard atmospheric conditions. Figure 5-1

	aerosol_cci2 ATBD (AATSR, ADV)	REF : ATBD – ADV ISSUE : 4.1 DATE : 21.04.2017 PAGE : XIX
---	---	--

shows an example of an AOD LUT. To ensure that the results of the radiative transfer computations are reliable the maximum value of sun and viewing zenith angles is limited to 75°.

Equation (4.8) shows that the computational task is to find the aerosol type mixture and reference AOD level that solve the equation for all three AATSR wavelengths simultaneously. Due to measurement and modeling errors this task is impossible in practice. Instead, the task can be converted to a least-squares type of problem

$$\arg_{b_1, L} \min \sum_{i=1}^{N_\lambda} \left[\frac{\rho^n(\lambda_i) - \rho_a^n(b_1, b_2, L, \lambda_i)}{T^n(b_1, b_2, L, \lambda_i)} - \frac{\rho^f(\lambda_i) - \rho_a^f(b_1, b_2, L, \lambda_i)}{kT^f(b_1, b_2, L, \lambda_i)} \right]^2, \quad (5.2)$$

where the fraction of the fine mode particles is $b_1 \in (0, 1)$, the non-absorbing component in fine particle mixture is $b_2 = b_{2,A} \pm 0.3$ with $b_2 \in (0, 1)$, and the reference AOD level is $L \in (1, 10)$. The mixture $b_{2,A}$ is the AEROCOM a priori value. Note that the dust fraction is not retrieved but the AEROCOM climatology value is used. The angle arguments (μ_1, μ, φ) have been omitted for brevity. The number of wavelengths $N_\lambda = 3$. Equation (5.2) also shows that the modeled atmospheric reflectance and transmittance are now functions of the decision arguments b_1, b_2 for aerosol component mixtures and L for the reference AOD level. The task is now to find the decision arguments (b_1, b_2, L) that minimize the least-squares sum.


The minimization problem (5.2) can be optimized by applying mathematical optimization methods. Here the chosen method is Levenberg-Marquardt (see for example [7]). It is a trust-region type method well suited for least-squares problems, and is meant for unconstrained optimization. The latter feature causes additional considerations as the decision arguments are all box-constrained. This is handled in the evaluation of the least-squares sum where strict barrier functions are used for constraining [7].

Another feature of the Levenberg-Marquardt method is that it is a local optimizer. It will converge efficiently to the nearest local minimum. To increase the probability of finding the globally best solution an initial search is done in a limited discrete set of decision parameters: ten mixtures b_1, b_2 , and ten AOD levels L . The results of the search are then used as the initial guess for the Levenberg-Marquardt method.

The k -ratio assumption of equation (4.6) works very well for AOD at an individual wavelength. When the AOD spectrum is investigated by computing the Ångström coefficient, however, it can be seen that aerosol models that have mainly or only small particles are favored too much. To correct this the k -ratio was then re-computed during the minimization of equation (5.2) to take into account the effect of coarse particles on the measured reflectance at 1.6 μm . This approach led to numerical instability in the mathematical Levenberg-Marquardt optimization. To compensate this instability an average of the original k -ratio, determined from the reflectance measurements, and the re-computed k -ratio is now used.

When all the decision parameters are set during the retrieval the resulting AOD τ can be computed from the LUTs:

$$\tau(\lambda) = b_1 [b_2 \tau_{naf}(\lambda, L) + (1 - b_2) \tau_{af}(\lambda, L)] + (1 - b_1) [b_{dust} \tau_{dust}(\lambda, L) + (1 - b_{dust}) \tau_{ss}(\lambda, L)], \quad (5.3)$$

	aerosol_cci2 ATBD (AATSR, ADV)	REF : ATBD – ADV ISSUE : 4.1 DATE : 21.04.2017 PAGE : XX
---	---	---

where the abbreviations are: naf – non-absorbing fine component, af – absorbing fine component, and ss – sea salt coarse component. Dust fraction b_{dust} is the above mentioned AEROCOM a priori value.

5.2 Over ocean implementation

In the ASV retrieval the same aerosol LUTs are used as for the ADV retrieval. Note that there is no distinction between land and ocean retrieval with respect to aerosol components. AEROCOM a priori values and retrieval itself decide the aerosol composition for any given pixel.

As was mentioned above the ASV method is based on minimizing the TOA measured and modelled reflectance. This leads to a considerably different minimization scheme from the one in ADV which can be seen in equation (5.2). The biggest physical difference is that only one of the AATSR views is used. Currently the forward view is employed as it is less hindered by sun glint than the nadir view. The minimization in the ASV problem, following the ADV notation, is

$$\arg_{b_1, b_2, L} \min \sum_{i=1}^{N_\lambda} [\rho^f(\lambda_i) - \rho_{\text{TOA}}^f(b_1, b_2, L, \lambda_i)]^2, \quad (5.4)$$

with the modifications that the number of wavelengths is now four as the 0.865 μm wavelength is also used, and modelled TOA reflectance is now the combined atmospheric and ocean surface reflectance.

When the ATSR2 and AATSR over ocean retrievals for the overlapping period (2002 - 2003) were compared it was found that the ATSR2 global average of the retrieved AOD values at 555 nm were about 0.03 higher than the values from the AATSR retrieval. Further investigation revealed that this difference is most probably due to the difference in the measured reflectance at the 555 nm wavelength. To harmonize the data sets, the 555 nm wavelength reflectance is currently not used in the ATSR2 over ocean retrieval. Note that even though a tiny difference can also be seen in the over land retrievals it is almost negligible as data from both views of the instruments are used which already compensates for the 555 nm reflectance difference.


5.3 Cloud screening

Clouded pixels have to be excluded from retrieval as they mask the other contributions of the atmosphere to the measured TOA reflectance. The tests that are described here were designed for the use with ATSR-2 data. For AATSR there are cloud flags included already in the reflectance data [1]. These flags were found to be too restricting: a significant amount of pixels that otherwise were giving good validation results were excluded. The use of these flags will be studied more in future.

Presently, three separate cloud screening tests are used. These tests are based on the work of [24] and [12]. To automate the cloud screening, AATSR orbits are divided into scenes of 480×512 pixels. Reflectance in each of the scenes is histogrammed and thresholds or rejection values for the tests are determined from the histograms. Since sun glinted pixels have very high reflectance values and this would potentially lead to unfeasible values for the thresholds, glinted pixels are omitted.

The automation of the tests is described by [22]. Brief description of the tests:

1. The gross cloud test. At the AATSR 12 μm brightness temperature channel clouds appear cooler than the underlying surface during day time. If the brightness temperature for a pixel is below threshold, the pixel is flagged as cloudy.

	aerosol_cci2 ATBD (AATSR, ADV)	REF : ATBD – ADV ISSUE : 4.1 DATE : 21.04.2017 PAGE : XXI
---	---	--

2. Generally, clouds are brighter than the underlying surface. If the reflectance of the 0.659 μm channel for a pixel is higher than threshold, the pixel is flagged as cloudy.
3. Ratio of the 0.865 and 0.659 μm reflectance. If the ratio is around one for a pixel, the pixel is flagged as cloudy. The distance from unity that governs cloud flagging is determined by the automation.

These tests are applied for both AATSR views. If any of the tests indicates that a pixel is clouded, it will be excluded from the retrieval.

5.4 Adaptation of ADV/ASV for global multi-year retrievals


The described ADV algorithm is suitable for retrieving the optical properties of aerosols over land as was demonstrated for several different areas by, e.g., [28, 30, 21, 23, 13, 25]. It became evident in the initial testing, however, that the time needed for retrieval computations was very long and processing of large data sets was very time consuming. The main reason was that two parameters need to be optimized during the retrieval process: the AOD reference level and the mixture of the two aerosol components. In addition, some statistical measures indicating the reliability of the retrieval can be computed using the ensemble of measured TOA reflectance values over a larger area. It was decided that for large retrieval tasks a larger result pixel size must be employed. This size was set to be $0.1^\circ \times 0.1^\circ$. In this section the methods for averaging the AATSR measured TOA reflectance over the larger pixel are described. Also the choice of aerosol models is discussed.

The natural assumption when averaging the TOA measured reflectance is that reflectance due to the atmosphere is sufficiently uniform over the averaged area. Here the term sufficient describes situations where sharp spatial gradients in aerosol conditions inside the area are not present. Reflectance due to atmospheric gases is assumed to be constant.

For the surface reflectance, however, this assumption can generally not be made. The complications in the averaging of the measured TOA reflectance are caused by the k -ratio approach of the ADV. The k -ratio is determined by applying equation (4.6) and using the nadir and forward view ground reflectance at 1.61 μm . It would be unrealistic to assume that ground reflectance is constant over the larger pixel area. In order to see how the k -ratio affects the retrieval process, equation (4.8) can be reformulated as

$$\frac{[\rho^f(\mu_1, \mu, \varphi, \lambda) - \rho_a^f(\mu_1, \mu, \varphi, \lambda)]/T^f(\mu_1, \mu, \varphi, \lambda)}{[\rho^n(\mu_1, \mu, \varphi, \lambda) - \rho_a^n(\mu_1, \mu, \varphi, \lambda)]/T^n(\mu_1, \mu, \varphi, \lambda)} = k. \quad (5.5)$$

It is evident that the value of k affects the results of retrieval strongly. If the k -ratio is computed using values that are simply averaged, values that are not representative for any of the pixels in the larger area could be most certainly encountered. For example, consider an area where half of the larger area is covered with pixels having a high and the other half having a low k -ratio. When the k -ratios are averaged the end result would be wrong for the ADV method. Furthermore, as both of the AATSR views are employed, in simple averaging of reflectance one cannot be certain that mutual nadir/forward pixels are used when the k -ratio is determined. This could lead to situations where, in principle, nadir and forward view reflectance come from different pixels.

	aerosol_cci2 ATBD (AATSR, ADV)	REF : ATBD – ADV ISSUE : 4.1 DATE : 21.04.2017 PAGE : XXII
---	---	---

The chosen approach to average measured reflectance is to find pixels that are the most representative for an area and at the same time are mutual to nadir and forward views. This is achieved by using the following method:

1. At least 50 % of the pixels belonging to an area must pass the cloud screening tests. This step ensures that enough information is present for the following steps.
2. Produce a histogram of the measured reflectance at 1.61 μm separately for nadir and forward reflectance. Typically seven bins are used ranging from zero to the maximum of the measured reflectance. The infrared channel is used here because the effect of aerosols is small. That is, the measured reflectance is considered in first approximation to have only surface contribution.
3. Choose the nadir/forward bins that have the maximum number of reflectance values.
4. Find out which pixels that are in the chosen bins are mutual to nadir and forward views.
5. If there are more than ten values left, average the chosen reflectance values and use them in retrieval. If less than ten values are left, the surface reflectance in the area is considered to vary too much and retrieval is not executed.

The number of bins in the histogram determination is a compromise between loss of data and degeneration towards simple averaging. If too many bins were used, there would be too few pixels for the averaging of the reflectance. This situation would be potentially poor in statistical sense when only few pixels would represent the whole area. If too few bins were used, too wide range of reflectance values would be accepted. This would allow pixels that could lead to a situation where the whole representative search of the *k*-ratio approach would become meaningless.


While *k*-ratio is used only for over land retrieval same principles for averaging are used also for over ocean. This is due to maintain a certain amount of uniformity between the two different retrieval types.

The other test for the averaged reflectance measures the sufficiently uniform atmosphere condition. The standard deviation of reflectance at 0.555 μm is used as a measure for the uniformity. The 0.555 μm channel is utilized here as it is sensitive to aerosol and cloud conditions. If the standard deviation is too large for an area, results are judged to be unreliable. Retrieval is still done and the results include the standard deviation which can then be applied by the end user to exclude unreliable areas. This test can be seen also as an additional spatial cloud screening but can also invalidate the pixel in case of strong aerosol gradients such as in the presence of strong sources. The current standard deviation threshold for excluding an area based on the 0.555 μm uniformity test is 0.009.

For the purpose of conforming to the aerosol_cci project, the results are finally mapped to $10 \times 10 \text{ km}^2$ sinusoidal grid (level 2 product). Results are also aggregated to a $1^\circ \times 1^\circ$ grid (level 3).

5.5 Post processing - Additional cloud screening

For each pixel retrieved with ADV a cloud post-processing test is applied to determine and discard the pixels that might potentially include cloud edge. Each pixel retrieved is analyzed together with the eight surrounding pixels in a $20 \times 20 \text{ km}^2$ area. If, in addition to the tested pixel, less than 3 pixels are retrieved in the area, the tested pixel is considered to be a cloud edge and discarded. If, besides tested pixel, at least 3 more pixels are retrieved and the

	<p>aerosol_cci2</p> <p>ATBD (AATSR, ADV)</p>	<p>REF : ATBD – ADV ISSUE : 4.1 DATE : 21.04.2017 PAGE : XXIII</p>
---	--	---

standard deviation of AOD for the pixels is more than 0.2, the tested pixel is discarded. For more detail see Kolmonen et al. (2016) [32].

The numbers presented above are a compromise between global coverage and acceptable validation results. However, for certain areas with high AOD (e.g. India, China), and for case studies of natural high AOD episodes (e.g. dust storms, volcanic eruptions), the limits for the AOD and standard deviation must be modified. For each 5 degrees in latitude part of the AATSR track "plume", or high AOD loading test is run. For that test a histogram is determined for the AOD retrieved. If number of AOD<0.6 pixels is lower than 40%, that 5 deg area is considered to be a high AOD loading episode and keep all the pixels retrieved. If the number of AOD<0.6 pixels is higher than 40%, post-processing is applied. More detail and examples are provided in Sogacheva et al. (2017) [33].



6 ERROR ESTIMATION

6.1 Error estimation for ADV

The effect of AATSR measurement error on AOD is described. First the uncertainty for the retrieved aerosol model decision parameters, which include the fine mode fraction b_1 , the absorbing/non-absorbing fine particle mixture b_2 , and the AOD level L , is determined. Then these errors are used to determine the uncertainty in the retrieved AOD.

The other possible sources for errors arise from modeling. These include uncertainty in the aerosol model selection (fine mode fraction, absorbing/non-absorbing fine particle mixture, dust fraction), LUT interpolation errors, and radiative transfer computation errors.

Formal treatment is based on the general equation formalism by Tarantola [26] (pp. 77 - 82). First, denote the parameters in the least squares problem (5.2) by

$$\mathbf{x} = \{b_1, b_2, L, r\}, \quad (6.1)$$

and the problem equations by

$$f_i(\mathbf{x}) = \frac{\rho^n(\lambda_i) - \rho^n(b_1, b_2, L, \lambda_i)}{T^n(b_1, b_2, L, \lambda_i)} - \frac{\rho^f(\lambda_i) - \rho^f(b_1, b_2, L, \lambda_i)}{kT^f(b_1, b_2, L, \lambda_i)}, \quad (6.2)$$



where $r = \{\rho^n(\lambda_i), \rho^f(\lambda_i)\} \forall i \in (1, 3)$ is the measured nadir and forward reflectance, b_1 is the fine mode fraction, b_2 is the absorbing/non-absorbing fine particle mixture, and L is the LUT AOD level. Index i refers to the wavelengths; $i = \{1, 2, 3\}$. Note that the dust fraction is not retrieved; it is taken from the AEROCOM climatology. This kind of formulation of the problem enables the determination of uncertainty for the decision parameters based on the measurement error. The formulation could take into account the effect of a priori information for b_1 , b_2 and L but this is neglected as the only error is assumed to come from the measurement.

Equation (13) can be solved in least-squares sense using a quasi-Newton method. The maximum likelihood point can be found using iteration

$$x_{n+1} = C_X + F_n^t (C_T + F_n C_X C_n^t)^{-1} f(x_n), \quad (6.3)$$

where

$$F_n = \left(\frac{\partial f}{\partial x} \right)_{x_n}. \quad (6.4)$$

A posteriori covariance is

$$C_{X'} = (F_\infty^t C_T^{-1} F_\infty + C_X^{-1})^{-1}, \quad (6.5)$$


where x_∞ is the solution of the minimized equation (6.3). Note that even though the ADV solution is not computed using the iteration scheme above it is still possible to determine the a posteriori covariance.

The Jacobian matrix F is of the form

$$F = \begin{pmatrix} \frac{\partial f_1}{\partial b_1} & \frac{\partial f_1}{\partial b_2} & \frac{\partial f_1}{\partial L} \\ \frac{\partial f_2}{\partial b_1} & \frac{\partial f_2}{\partial b_2} & \frac{\partial f_2}{\partial L} \\ \frac{\partial f_3}{\partial b_1} & \frac{\partial f_3}{\partial b_2} & \frac{\partial f_3}{\partial L} \end{pmatrix} \quad (6.6)$$

All the partial derivatives are computed numerically as the evaluation of these values requires interpolation from the aerosol LUTs and analytical differentiation is impossible.

The covariance CT is here consisted of only measurement errors. For AATSR this error is taken to be 5 % of the measured signal for the whole spectrum [27]. The principal difficulty is that in equation (6.3) there are two measured values $\rho^n(\lambda_i)$ and $\rho^f(\lambda_i)$. The formulation in equation (6.5), however, takes into account the uncertainty of only one value in the covariance matrix. The solution is that as the nadir and forward relative measurement error equal to the larger absolute value is used. It would be useful to study individually the effect of the nadir and forward measurement error on the aerosol model parameters in future. In addition, when all errors are considered to be Gaussian in nature, modeling errors could be simply added to the measurement errors [26]. Another simplification that is made here is that measurement errors

	aerosol_cci2 ATBD (AATSR, ADV)	REF : ATBD – ADV ISSUE : 4.1 DATE : 21.04.2017 PAGE : XXVI
---	---	---

do not correlate. Thus, C_T is diagonal. This assumption does not hold true for the a posteriori covariance C_X' . The uncertainty in the aerosol model parameters will be correlated.

The a priori covariance matrix for the aerosol model defining parameters C_X is neglected at the moment as the uncertainty contribution of the measurement error to these very parameters is the motivation of this treatment.

AOD is determined for each three wavelengths using the aerosol model defined by the three optimized decision parameters: b_1 , b_2 and L . First, for all four aerosol types that are used the corresponding AOD is interpolated from their LUTs by using the AOD level parameter L . Then, simultaneously, fine aerosol type is mixed from the non-absorbing and absorbing AOD using b_2 , and coarse aerosol type is mixed from the sea salt and dust AOD using the dust fraction. The final AOD is then mixed from the fine and coarse AOD using b_1 ; see equation (5.3).

Denote the AOD interpolation/mixing operator by p . Then for wavelength i AOD is


$$AOD_i = p_i(b_1, b_2, L). \quad (6.7)$$

The covariance of AOD is then

$$CAOD = PC_X' P^t, \quad (6.8)$$

where P is now the Jacobian of the interpolation/mixing operator

$$P = \begin{pmatrix} \frac{\partial p_1}{\partial b_1} & \frac{\partial p_1}{\partial b_2} & \frac{\partial p_1}{\partial L} \\ \frac{\partial p_2}{\partial b_1} & \frac{\partial p_2}{\partial b_2} & \frac{\partial p_2}{\partial L} \\ \frac{\partial p_3}{\partial b_1} & \frac{\partial p_3}{\partial b_2} & \frac{\partial p_3}{\partial L} \end{pmatrix} \quad (6.9)$$

	aerosol_cci2 ATBD (AATSR, ADV)	REF : ATBD – ADV ISSUE : 4.1 DATE : 21.04.2017 PAGE : I
---	---	--


For reference, see e.g. [15]. The uncertainty estimate for AOD can be finally found in the diagonal of CAOD.

The uncertainty of the dust fraction, which is not a retrieved parameter, could be added to CX' if this uncertainty was assumed to be Gaussian.

6.2 Error estimation for ASV

The effect of AATSR measurement error on the retrieved AOD was already described for the ADV algorithm. This error treatment can be straightforwardly applied for the ASV algorithm by replacing equation (13) with the ASV minimization from equation (27):

$$f_i(x) = \rho^f(\lambda_i) - \rho_{\text{TOA}}^f(b_1, b_2, L, \lambda_i). \quad (6.10)$$

	aerosol_cci2 ATBD (AATSR, ADV)	REF : ATBD – ADV ISSUE : 4.1 DATE : 21.04.2017 PAGE : II
---	---	---

7. INPUT DATA REQUIREMENTS

Here the input data for ADV/ASV are described.

7.1 AATSR reflectance

The AATSR Gridded Brightness Temperature/Reflectance (ATS_TOA_1P) is used for measured reflectance at the wavelengths of (0.555, 0.659, 0.865, and 1.610 μm). Brightness temperature at 12 μm is utilized in cloud screening. In addition the 3.7 and 11 μm channels are read into the algorithm. Glint flag, that is provided in the data is used to exclude glinted pixel in over ocean retrieval.

7.2 Aerosol look-up-tables (LUTs)


LUTs are pre-calculated and stored in HDF version 4.2 format.

7.3 Chlorophyll concentration

The concentration is a binary file consisting of the global chlorophyll data from Coastal Zone Color Scanner (CZCS).

7.4 Monthly wind speed climatology


The climatology is based on SAR satellite imagery and is described by Monado et. al. [17].

	aerosol_cci2 ATBD (AATSR, ADV)	REF : ATBD – ADV ISSUE : 4.1 DATE : 21.04.2017 PAGE : III
---	---	--

8. ALGORITHM OUTPUT

Results in the NetCDF-formatted product are given at two ground resolutions:

- Level 2 product for each orbit. $10 \times 10 \text{ km}^2$ ground sinusoidal resolution. For each retrieved pixel:
 - Coordinates (lat/lon).
 - AOD at 0.555, 0.659, and 1.610 μm over land.
 - AOD at 0.555, 0.659, 0.865, and 1.610 μm over ocean.
 - Uncertainties for the AOD values (excluding AOD at 0.865 μm).
 - Quality indicator based on the 0.555 μm variance in reflectance (described above).
 - Angstrom coefficient computed with AODs at 0.555/0.659 μm and AODs at 0.555/0.659/1.610 μm .
 - Time in Julian Unix.
 - Measurement geometry (solar/viewing zenith angles and relative azimuth angles for both AATSR views (nadir/forward)).
 - Cloud fraction.
 - Fraction of water.
- Level 3 product daily. $1^\circ \times 1^\circ$ ground resolution. For each aggregated pixel:
 - Coordinates (lat/lon).
 - Mean AOD at 0.555, 0.659, and 1.610 μm over land and ocean.
 - Standard deviation of AOD at 0.555, 0.659, and 1.610 μm over land and ocean.
 - Aggregated quality indicator.
 - Number of level 2 results used in the aggregation.

	aerosol_cci2 ATBD (AATSR, ADV)	REF : ATBD – ADV ISSUE : 4.1 DATE : 21.04.2017 PAGE : IV
---	---	---

9. PRACTICAL CONSIDERATIONS FOR IMPLEMENTATION

9.1 The retrieval algorithm

The ADV algorithm is implemented using Fortran 90 and C languages. The algorithm is compiled with gfortran and gcc compilers under Linux Ubuntu and Fedora operating systems. Currently the algorithm is run in Linux PC environment. It has been tested and run at FMI (Finnish meteorological Institute) server.

The retrieval of one month of global AOD takes about 6 days using a PC with Intel Core2 Duo CPU E8400 at 3.00 GHz. The usage of RAM is well beyond 1 GB.

Additional Linux scripts are used for AATSR data access (rolling archive ftp and local server scp), launching the retrieval algorithm, and possible data upload (scp).

9.2 Look-up-table (LUT) computation

LUTs are computed by using Fortran 77 implementations of Mie and radiative transfer algorithms. Currently computations are run in Linux PC environment with gfortran compiler.



aerosol_cci2
ATBD (AATSR, ADV)

REF : ATBD – ADV
ISSUE : 4.1
DATE : 21.04.2017
PAGE : V

10. CONCLUSIONS

The ADV/ASV retrieval method was described. The method is capable of retrieving AOD globally over land and ocean.

The method is under constant development and the description here has to be considered not as a final product description but as a report of the current state of the development.



aerosol_cci2
ATBD (AATSR, ADV)

REF : ATBD – ADV
ISSUE : 4.1
DATE : 21.04.2017
PAGE : VI

End of the document